Published for SISSA by Springer

Received: *September 19, 2013*
Accepted: *January 8, 2014*
Published: *February 14, 2014*

Holographic superfluids and the Landau criterion

Irene Amado,[a] **Daniel Areán,**[b,c] **Amadeo Jiménez-Alba,**[d] **Karl Landsteiner,**[d] **Luis Melgar**[d] **and Ignacio Salazar Landea**[e,b]

[a] *Department of Physics, Technion, Israel Institute of Technology, Haifa 32000, Israel*
[b] *International Centre for Theoretical Physics (ICTP), Strada Costiera 11; I 34014 Trieste, Italy*
[c] *INFN — Sezione di Trieste, Strada Costiera 11; I 34014 Trieste, Italy*
[d] *Instituto de Física Teórica IFT-UAM/CSIC, Universidad Autónoma de Madrid, C/ Nicolás Cabrera 13-15, 28049 Cantoblanco, Spain*
[e] *Instituto de Física La Plata (IFLP), and Departamento de Física, Universidad Nacional de La Plata, CC 67, 1900 La Plata, Argentina*

E-mail: irene.r.amado@gmail.com, arean@sissa.it, amadeo.j@gmail.com, karl.landsteiner@csic.es, luis.melgar@csic.es, peznacho@gmail.com

Abstract: We revisit the question of stability of holographic superfluids with finite superfluid velocity. Our method is based on applying the Landau criterion to the Quasinormal Mode (QNM) spectrum. In particular we study the QNMs related to the Goldstone modes of spontaneous symmetry breaking with linear and quadratic dispersions. In the linear case we show that the sound velocity becomes negative for large enough superfluid velocity and that the imaginary part of the quasinormal frequency moves to the upper half plane. Since the instability is strongest at finite wavelength, we take this as an indication for the existence of an inhomogeneous or striped condensed phase for large superfluid velocity. In the quadratic case the instability is present for arbitrarily small superfluid velocity.

Keywords: AdS-CFT Correspondence, Holography and quark-gluon plasmas, Holography and condensed matter physics (AdS/CMT)

ArXiv ePrint: 1307.8100

doi:10.1007/JHEP02(2014)063

JHEP02(2014)063

Contents

1 Introduction

The characteristic property of a superfluid is its ability to flow totally frictionless through thin capillaries. It is useful to think of a superfluid as a two component liquid. One component is the ground state with a macroscopic occupation number and the other is the normal component, subject to friction and viscosity. At very low temperatures the normal component can be described as the gas of elementary quasi particle excitations above the macroscopically occupied ground state. A famous argument due to Landau [1–3] sets a limit to the flow velocity that the condensate can obtain. The essence of the argument is as follows. At zero temperature the energy of a quasiparticle excitation of momentum $\vec{p}$ is $\epsilon(\vec{p})$ in the rest frame of the condensate. If we imagine a situation in which the condensate moves with constant velocity $\vec{v}$ the energy cost in creating a quasiparticle is

$$\epsilon'(\vec{p}) = \epsilon(\vec{p}) + \vec{v}\cdot\vec{p}\,. \tag{1.1}$$

In particular if $\vec{p}$ is anti-parallel to the flow velocity $\vec{v}$ this energy is diminished and eventually goes to zero. If $\epsilon' < 0$ it is energetically favorable for the system to create elementary excitations and populate states with this effective negative energy. Since the superfluid velocity $\vec{v}$ is kept constant this means that eventually the condensate gets completely depleted and the superflow stops. It follows that there is a critical flow velocity above which the superfluid ceases to exist. The famous Landau criterion for the existence of superflow is therefore

$$v_{\rm max} = \min \frac{\epsilon(p)}{p}\,, \tag{1.2}$$

JHEP02(2014)063

where the minimum over all elementary excitation branches has to be taken. It is known for example for superfluid helium that the low temperature normal component can be well described as a gas of phonons and rotons and that the critical velocity is not determined by the minimum of the phonon and roton dispersion relation but rather by the excitation of vortices, resulting in a much lower critical velocity.

At higher temperatures there is always a normal component present and therefore the energy of an excitation of a superfluid with superflow can not be obtained by a (Galilean) boost as in equation (1.1). It is however still true that the energy will depend on the superfluid velocity and that it can become negative if the superfluid velocity is too large. At finite temperature the criterion is therefore that the superflow is stable as long as the energy of all quasiparticle excitations is positive. If in a superfluid the only low energy excitations are the phonons that criterion is basically the statement that the superflow dependent sound velocity is positive for all directions.

The AdS/CFT correspondence has proven to be a very useful tool for studying quantum field theories at strong coupling. In particular, since we can study Bose and Fermi systems at finite temperature and chemical potential using holography, there are many condensed matter physics applications of the duality (for a review, see [4–6]).

One of the most important achievements of AdS/CMT in the last years is the construction of geometries dual to superfluids [7–9]. The order parameter can be either a scalar, a vector or a spin-2 tensor (we talk of s-, p- [10, 11] and d-wave superfluidity [12, 13], respectively).

In [14, 15] an s-wave superfluid in 2+1 dimensions with superflow was constructed and it was pointed out that there is indeed a critical velocity above which the superfluid state ceases to exist. The phase diagram obtained in these works was based on comparing the free energy of the superflow with the free energy of the normal phase. It turned out that the phase transition from the superfluid phase to the normal phase was either first or second order depending on the temperature. Remarkably enough, in 3+1 dimensions there is some range of masses of the condensate for which the phase transition is always of second order type [16]. Another way of establishing the phase diagram has been used in [17]. There the supercurrent was fixed and it was argued that the phase transition is always first order.

The physical significance of the comparison of the free energies of the state with superflow and the normal state is not totally clear, since for all temperatures below the critical temperature the normal state is unstable towards condensation to the superfluid state without superflow. Indeed the superflow by itself is a metastable state only [3] as emphasized already in [14]. We will propose a different method of characterizing the phase diagram more directly related to the stability criterion (1.2).

The purpose of this paper is thus to revisit the question of the realization of the stability criterion (1.2) in holographic superfluids. The simplest holographic models of superfluids are obtained in the so called decoupling limit. In this limit one discards the fluctuations of the metric and keeps only the dynamics of a charged scalar field and a gauge field in an asymptotically AdS black hole. The excitation spectrum of a holographic field theory at finite temperature and density is given by the spectrum of quasinormal modes (QNMs) [18–

JHEP02(2014)063

21]. The QNMs of the simplest holographic superfluid with a spontaneously broken U(1) symmetry have been obtained in [22]. Recently this model has been generalized to a case with U(2) symmetry [23],[1] giving rise to the holographic dual of a multi-component fluid [25]. The spectrum of the U(2) model turned out to contain a copy of the usual QNM spectrum of the U(1) model but also a novel feature, the appearance of a type II Goldstone boson.

It is of course a standard fare that the breaking of a continuous symmetry leads to the appearance of ungapped states, the Goldstone bosons. This is also respected by holographic field theories. The Goldstone bosons appear as special ungapped QNMs. It is less well-known that Goldstone bosons do not necessarily have linear dispersion relation even in relativistic field theories. Depending on whether their dispersion relation is proportional to an odd or even power of the momentum they are called of type I or of type II (see [26] for a review). The appearance of type II Goldstone bosons is also related to another fact, namely that the number of Goldstone bosons does not equal the number of broken generators [27–29].[2] In fact in the holographic model the U(2) symmetry gets broken to U(1) and consequently there are three broken symmetry generators but only two holographic Goldstone bosons were found. One of them could be identified with the usual sound mode with linear dispersion relation

$$\omega(k) = v_s k + (b - i\Gamma)k^2, \tag{1.3}$$

where v_s is the speed of sound, b a correction quadratic in momentum and Γ the sound attenuation constant. The type II Goldstone boson on the other hand was found to have dispersion relation

$$\omega(k) = (B - iC)k^2, \tag{1.4}$$

with no linear part. All the constants appearing in these dispersion relations are of course temperature dependent and obey $v_s(T_c) = 0$, $b(T_c) = B(T_c)$ and $C(T_c) = \Gamma(T_c)$.

We will investigate the stability of the superflow via a QNM analysis of the U(2) model. This automatically will give new and valuable information about the usual U(1) holographic superfluid since a subsector of the linear fluctuations in the U(2) model is isomorphic to it.

In section two we will follow [14, 15] and reproduce the phase diagram based on the comparison of the free energy of the superflow with the normal phase. Then we will study the QNM spectrum with the superflow. In particular we will calculate the direction dependent speed of sound. We will indeed find that as the superfluid velocity is increased the speed of sound in opposite direction to the superflow is diminished and eventually vanishes at a critical velocity v_c. Increasing the superfluid velocity even further this sound velocity becomes negative and this has to be interpreted as the appearance of a negative energy state in the spectrum. In principle that would be enough to argue for instability but at basically no price the QNM analysis can give us an even clearer sign of instability.

[1] This holographic model has also been introduced in [24].

[2] Further recent results on type II Goldstone bosons can be found in [30–33]. In a holographic context type II Goldstone bosons have been also found previously in [34].

JHEP02(2014)063

It is well-known that the imaginary part of the QNMs have to lie all in the lower half plane. If they fail to do so an exponentially growing mode with amplitude $\phi \propto \exp(\Gamma t)$ appears in the spectrum. It is not necessary for this mode to have zero momentum. In fact we will see that if we increase the superfluid velocity beyond the critical value the imaginary part of the sound mode quasinormal frequency moves into the upper half plane. And it does so attaining a maximum for non-zero momentum. We will see that this behavior is necessary to connect the phase diagram continuously to the normal phase. Then moving slightly aside we will study the conductivities with superflow. This has been done before but only in the transverse sector and here we present results for the longitudinal sector.

Finally we will briefly investigate the fate of the type II Goldstone mode in the U(2) model. We will study both the gauged and the ungauged model of [23]. Landau's criterion suggests that these setups do not sustain any finite superflow since $\min \frac{\epsilon(p)}{p} = 0$ for quadratic dispersion relations. Again we can not only look at the real part but also at the imaginary part. We will indeed find poles in the upper half plane for non-zero momenta for all temperatures and superfluid velocities for the gauged and the ungauged model.[3]

Let us also mention some shortcomings of our analysis. We always work in the so-called decoupling limit in which the metric fluctuations are suppressed. Therefore we do not see the pattern of first and second (and fourth) sound typical for superfluids. In the decoupling limit only the fourth sound, the fluctuations of the condensate, survive. Another shortcoming is that we can apply the Landau criterion only to the QNMs. As in superfluid Helium there exist most likely other excitations, such as vortices, that might modify the value of the critical velocity. The question of if and how solitons of holographic superfluids determine the critical superfluid velocity has been investigated in [38].

It is interesting to compare our results to the direction dependence of the sound velocities in a weakly coupled model like the one recently studied in [39].

2 The U(2) superfluid with superflow

Consider the bulk Lagrangian for a complex scalar field in the fundamental representation of a U(2) gauge symmetry [23, 24]

$$S = \int d^4x\sqrt{-g}\mathcal{L} = \int d^4x\sqrt{-g}\left(-\frac{1}{4}F^{\mu\nu c}F^c_{\mu\nu} - m^2\psi^\dagger\psi - (D^\mu\psi)^\dagger D_\mu\psi\right), \tag{2.1}$$

where

$$\psi = \sqrt{2}\begin{pmatrix}\lambda\\ \Psi\end{pmatrix}, \qquad A_\mu = A^c_\mu T_c\,, \qquad D_\mu = \partial_\mu - iA_\mu\,, \tag{2.2}$$

where we include the $\sqrt{2}$ in the definition of the scalar field to agree with the equations of [14]. Following [8] we choose the mass of the scalar field to be $m^2 = -2/L^2$. We take the generators of U(2) to be

$$T_0 = \frac{1}{2}\mathbb{I}\,, \qquad T_i = \frac{1}{2}\sigma_i\,. \tag{2.3}$$

[3] Models with one U(1) gauge field and two complex scalars similar to our ungauged model were studied before in [35] and recently in [36] (see also [37]). There the two scalars had however different masses and this should prevent the appearance of the ungapped type II Goldstone mode.

JHEP02(2014)063

Since we will work in the probe approximation we do not include the metric in the dynamical degrees of freedom but simply consider (2.1) in the background metric of the Schwarzschild-AdS black brane

$$ds^2 = -f(r)dt^2 + \frac{dr^2}{f(r)} + \frac{r^2}{L^2}(dx^2 + dy^2)\,,$$
$$f(r) = \frac{r^2}{L^2} - \frac{M}{r}\,. \tag{2.4}$$

The horizon is located at $r_H = M^{1/3}L^{2/3}$ and its Hawing temperature is $T = 3r_H/4\pi L^2$. By suitable rescalings we can set $L = r_H = 1$ and work with dimensionless coordinates.

In order to find background solutions corresponding to a condensate with non-vanishing superfluid velocity we proceed as follows. First note that the scalar field $\lambda(r)$ can be set to zero by a U(2) gauge transformation. For the scalar Ψ we demand then that the non-normalizable mode vanishes. By a residual U(1) gauge transformation we can also take Ψ to be real.

Now we need to define what we mean by the superflow. Let us discuss this for a moment from a field theory perspective. In a multi-component superfluid with U(2) symmetry we can in principle construct the four (super) currents

$$J^\mu_a = \Phi^\dagger T_a \nabla^\mu \Phi - (\nabla^\mu \Phi)^\dagger T_a \Phi\,, \tag{2.5}$$

where $\nabla^\mu = \partial^\mu - iA^\mu_a T_a$ is the covariant derivative and Φ is the condensate wave function which transforms as a doublet under U(2). If the condensate is such that one of the spatial currents does not vanish we can speak of a state with non-vanishing superflow. By a gauge transformation we can always assume the condensate to take some standard form, e.g. $\Phi = (0, \phi)^T$ and represent the non-vanishing superflow in terms of constant gauge fields. Since we are interested in the case where we break the U(2) symmetry spontaneously to U(1) we will only allow a non-zero gauge field in the overall U(1) corresponding to the generator T_0. Furthermore by an SO(2) rotation we can take the gauge field to point into the x direction. From (2.5) it is easy to see that such a superflow has non-vanishing currents $J^{(0)}_x$ and $J^{(3)}_x$. In order to find solutions with non-trivial charge we also need to introduce a chemical potential. Again in order to preserve the full U(2) symmetry we also allow a chemical potential only for the overall U(1) charge.

Returning now to Holography these considerations determine the ansatz for the gauge fields to be of the form

$$A^{(0)} = A^{(0)}_t(r)dt + A^{(0)}_x(r)dx\,, \qquad A^{(3)} = A^{(3)}_t(r)dt + A^{(3)}_x(r)dx\,. \tag{2.6}$$

While we introduce sources only for $A^{(0)}$ the fact that also the current $J^{(3)}_\mu$ is nonvanishing demands that $A^{(3)} \neq 0$. The physical interpretation for this fact is that the system forces the appearance of a charge density $\rho^{(3)} \neq 0$ (as noticed already in [23]) and a current $J^{(3)}_x$ in the vacuum with superflow. This is in turn closely related to the presence of type II Goldstone bosons in the spectrum [40].

JHEP02(2014)063

At this point it is important to note that the above identification is only valid in the superfluid phase, that is, whenever $\Psi \neq 0$. A constant background value of the gauge field A_x in the normal phase is not physically meaningful since there is no notion of superflow.

For the reasons outlined above we choose the asymptotic boundary conditions for the gauge fields to be

$$\begin{aligned} A_t^{(0)}(r \to \infty) &= 2\bar{\mu}\,, & A_t^{(3)}(r \to \infty) &= 0\,, \\ A_x^{(0)}(r \to \infty) &= 2\bar{S}_x\,, & A_x^{(3)}(r \to \infty) &= 0\,, \end{aligned} \tag{2.7}$$

where $\bar{\mu}$ is to be identified with the chemical potential of the dual theory and $\bar{S}_x$ is related to the superflow velocity. We have included a factor of two in the definitions of $\bar{\mu}$ and $\bar{S}_x$ for the following reason. The background field equations can be recast in the form of those derived from the U(1) model in [14, 15] by using the field redefinitions

$$\begin{aligned} A_0 &= \frac{1}{2}(A_t^{(0)} - A_t^{(3)})\,, & \xi &= \frac{1}{2}(A_t^{(0)} + A_t^{(3)})\,, \\ A_x &= \frac{1}{2}(A_x^{(0)} - A_x^{(3)})\,, & \varsigma &= \frac{1}{2}(A_x^{(0)} + A_x^{(3)})\,, \end{aligned} \tag{2.8}$$

for which the background equations now read

$$\Psi'' + \left(\frac{f'}{f} + \frac{2}{r}\right)\Psi' + \left(\frac{A_0^2}{f^2} - \frac{A_x^2}{r^2 f} - \frac{m^2}{f}\right)\Psi = 0\,, \tag{2.9}$$

$$A_0'' + \frac{2}{r}A_0' - \frac{2\Psi^2}{f}A_0 = 0\,, \tag{2.10}$$

$$A_x'' + \frac{f'}{f}A_x' - A_x\frac{2\Psi^2}{f} = 0\,, \tag{2.11}$$

$$\xi'' + \frac{2}{r}\xi' = 0\,, \tag{2.12}$$

$$\varsigma'' + \frac{f'}{f}\varsigma' = 0\,. \tag{2.13}$$

It can be checked that we recover the usual U(1) system describing the U(1) holographic superconductor in the presence of superfluid velocity (see for instance [16]). The chemical potential $\bar{\mu}$ is therefore the chemical potential for the field A_0 which plays the role of the temporal component of the (single) gauge field, and A_x plays the role of the spatial component of the single gauge field of [14–16]. This explicitly shows that the background of the U(2) model is identical to that of the U(1) superconductor, even for a nonzero superfluid velocity.

An immediate consequence of the fact that the background equations are those of the U(1) holographic superfluid is that, at first sight, the U(2) system seems to be able to accommodate a superflow. However, as already argued, this is in direct contradiction with the Landau criterion of superfluidity [3] due to the presence of a type II Goldstone in the spectrum. Of course, having found solutions to the equations of motion does not yet say anything about the stability. In fact as we will explicitly see the type II Goldstone will turn into an unstable mode and therefore make the whole U(2) solution with superflow unstable.

JHEP02(2014)063

Equations (2.9)–(2.11) are non-linear and have to be solved using numerical methods. Notice that (2.12) and (2.13) are decoupled. They correspond to the preserved U(1) symmetry after having broken spontaneously U(2) → U(1). The asymptotic behavior of the fields close to the conformal boundary is

$$\begin{aligned} A_0 &= \bar{\mu} - \frac{\bar{\rho}}{r} + \dots , \\ A_x &= \bar{S}_x - \frac{\bar{\mathcal{J}}_x}{r} + \dots , \\ \Psi &= \frac{\psi_1}{r} + \frac{\psi_2}{r^2} + \dots . \end{aligned} \tag{2.14}$$

The asymptotic quantities are related to the physical ones by

$$\begin{aligned} \bar{\mu} &= \frac{3}{4\pi T}\mu , & \bar{\rho} &= \frac{9}{16\pi^2 T^2}\rho , \\ \bar{S}_x &= \frac{3}{4\pi T}S_x , & \bar{\mathcal{J}}_x &= \frac{9}{16\pi^2 T^2}\mathcal{J}_x , \\ \psi_1 &= \frac{3}{4\pi T}\langle \mathcal{O}_1 \rangle , & \psi_2 &= \frac{9}{16\pi^2 T^2}\langle \mathcal{O}_2 \rangle . \end{aligned} \tag{2.15}$$

We are working in the grand canonical ensemble, then we fix the chemical potential μ. The temperature is defined by $T/\mu \propto 1/\bar{\mu}$. For studying the evolution of the condensate as a function of the superfluid velocity, the natural way to proceed is to work with S_x/μ as our free parameter together with temperature. Notice that both asymptotic modes of the scalar field are actually normalizable [41]. From now on we will stick to the $\mathcal{O}_2$ theory, for which $\psi_1 = 0$ and $\langle \mathcal{O}_2 \rangle$ is the vev of a scalar operator of mass dimension two in the dual field theory. Notice that the fields ξ and ζ corresponding to the unbroken U(1) are given by

$$\begin{aligned} \xi &= \bar{\mu} - \bar{\rho}/r , \\ \zeta &= \bar{S}_x , \end{aligned} \tag{2.16}$$

even with non-vanishing condensate.

The values of the condensate as a function of temperature and superfluid velocity shown in figure 1 reproduce the previous results of [14, 15]. In the plot and in the rest of the paper the temperature is measured with respect to the critical temperature of the phase transition with no superfluid velocity, i.e. $T_c \approx 0.0587\mu$.

2.1 Free energy

In this section we compute the free energy of the condensed phase and compare it to the free energy of the unbroken phase as done in [14, 15]. After appropriate renormalization of the Euclidean on-shell action and using the boundary conditions (2.14), the free energy density reads

$$F = -TS_{\text{ren}} = -\bar{\mu}\bar{\rho} + \bar{S}_x\bar{\mathcal{J}}_x + \int_1^\infty dr \left(\frac{2r^2 A_0^2}{f} - 2A_x^2 \right) \Psi^2 . \tag{2.17}$$

JHEP02(2014)063

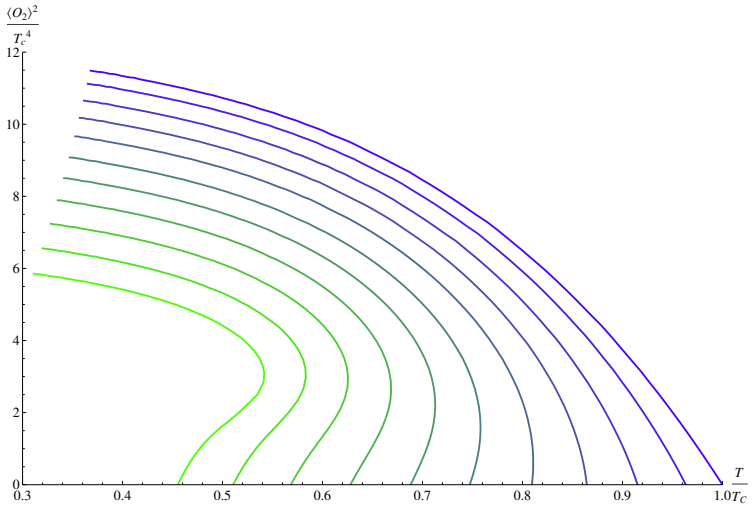

Figure 1. The condensate for different values of the superfluid velocity, ranging from $\frac{S_x}{\mu} = 0.005$ (right) to $\frac{S_x}{\mu} = 0.530$ (left).

In the normal phase $\Psi = 0$, regularity at the horizon forces the A_x gauge field to have a trivial profile along the radial direction in the bulk and therefore not to contribute to the free energy, i.e. $\bar{\mathcal{J}}_x = 0$. This is in accordance with the fact that in absence of a scalar condensate it is not possible to switch on a superfluid velocity anymore. Switching on the spatial component of the gauge field in the normal phase describes a pure gauge transformation that does not affect the free energy of the system. In the broken phase instead, different superfluid velocities are physically distinguishable. It is important to emphasize that one is actually comparing the normal phase at vanishing superfluid velocity with the superconducting phase at different values of the superfluid velocity, and that the normal phase is unstable towards condensation without superflow for any $T < T_c$. Therefore, the physical relevance of this comparison is not completely clear. We will see later on that actually the Landau criterion establishes a different transition temperature for the superfluid phase. Nevertheless the free energy gives a natural first approach to characterize the phase diagram of the system. We would like to remark that the superflow phase is just a metastable phase, since the true background is the static condensed phase which allways has lower free energy [3, 14].

In figure 2 the free energy of both the normal and condensate phase is plotted for different values of $\frac{Sx}{\mu}$. The different behavior for large and small values of the superfluid velocity is apparent. For large superfluid velocity the transition is first order as can be seen from the left panel in figure 2, indicated by the open circle. Coming from low temperatures the system can still be overheated into a metastable state until the point of spinodal decomposition where the order parameter susceptibility $\partial\langle\mathcal{O}\rangle/\partial\mu$ diverges, indicated by the filled circle.

For low superfluid velocities the normal phase free energy and the condensate free energy match smoothly at a second order phase transition. The resulting phase space is contained in figure 6 and reproduces the previous analysis in [14, 15].

JHEP02(2014)063

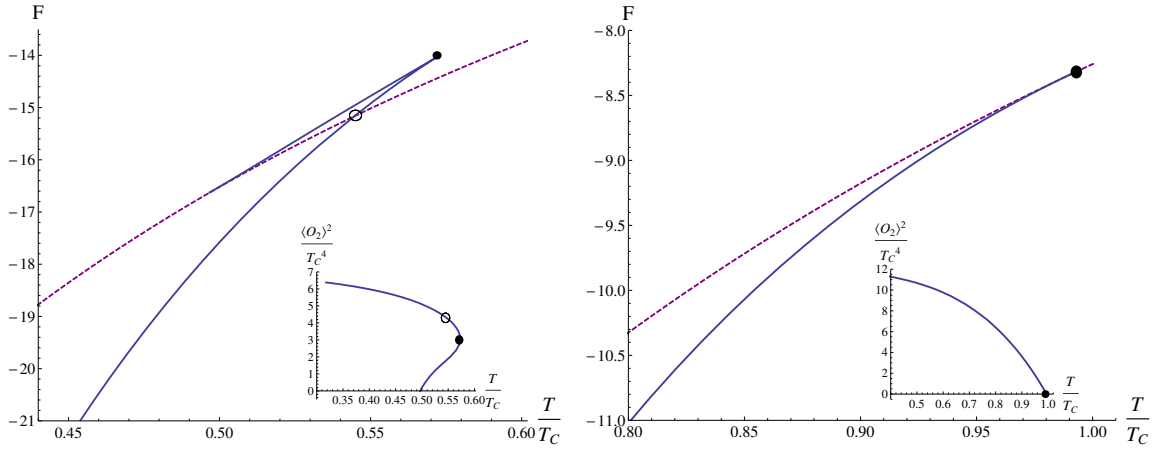

Figure 2. Free energy of the condensed (solid line) and normal (dashed line) phases for $\frac{S_x}{\mu} = 0.5$ (left) and $\frac{S_x}{\mu} = 0.05$ (right). The small plots show the behavior of the condensate. The open circle corresponds to the critical temperature $\tilde{T}$ whereas the filled circle corresponds to the spinodal point (max. overheating).

The phase transition found from considerations of the free energy is however only apparent. We will call the temperature at which the free energies of the condensate phase with superflow and the free energy of the normal phase coincide $\tilde{T}$ from now on. The temperature at which the (second order) phase transition occurs without superflow we will denote by T_c. As we will show now the superflow becomes unstable at temperatures below $\tilde{T}$ as implied by the Landau criterion applied to the sound mode. This temperature we will denote by T^*.

3 Landau criterion for the U(1) sector

In this section we analyze the QNM spectrum of the (0)–(3) sector, which is identical to the original U(1) holographic superconductor in the presence of superfluid velocity [14, 15]. We focus on the behavior of the lowest QNM, the type I Goldstone boson, with special emphasis on the velocity and the attenuation constant and their dependence on the superfluid velocity and on the angle of propagation with respect to the flow.

To study the QNM spectrum we consider linearized perturbations around the background of the fields of the form $\delta\phi_I = \delta\phi_I(r)\exp[-i(\omega\, t - |k|\, x\cos(\gamma) - |k|\, y\sin(\gamma)]$. Specifically we consider the fluctuations

$$\begin{aligned} \delta\hat{\Psi}^T &= \big(\eta(r), \sigma(r)\big)\,, \\ \delta A^{(0)} &= a_t^{(0)}(r)dt + a_x^{(0)}(r)dx + a_y^{(0)}(r)dy\,, \\ \delta A^{(3)} &= a_t^{(3)}(r)dt + a_x^{(3)}(r)dx + a_y^{(3)}(r)dy\,, \end{aligned} \tag{3.1}$$

where in the case of the gauge fluctuations we will work with the linear combinations already defined by (2.8), i.e. $a_\mu^{(-)} \equiv \frac{1}{2}(a_\mu^{(0)} - a_\mu^{(3)})$ and $a_\mu^{(+)} \equiv \frac{1}{2}(a_\mu^{(0)} + a_\mu^{(3)})$. The linearized equations are rather complicated and we list them in appendix A. The numerical techniques

JHEP02(2014)063

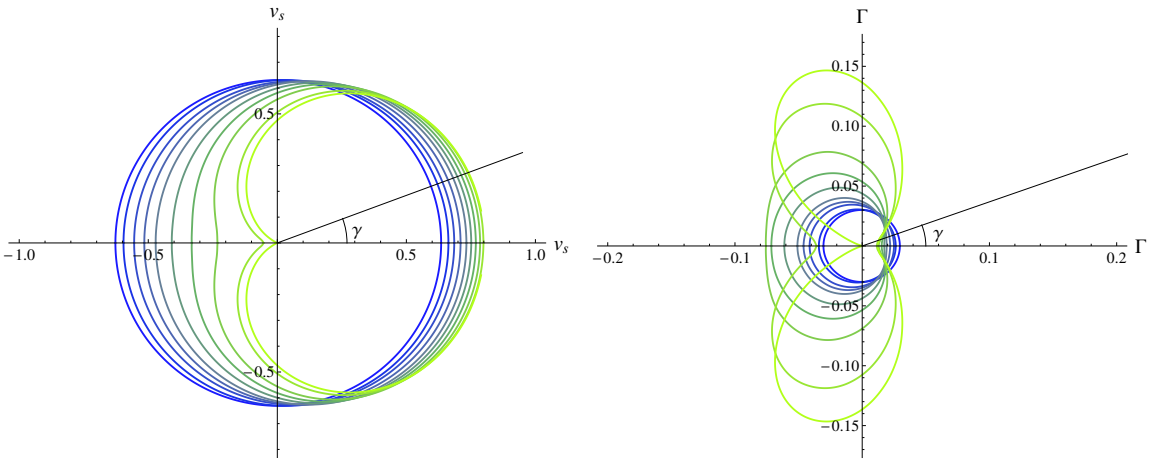

Figure 3. Sound velocity and damping for $T = 0.7T_c$ and several superfluid velocities from $S_x/\mu = 0$ (blue) to $S_x/\mu = 0.325$ (green). The radius represents the absolute value of the sound velocity (left) and attenuation constant (right) as a function of the angle γ between the momentum and the superfluid velocity.

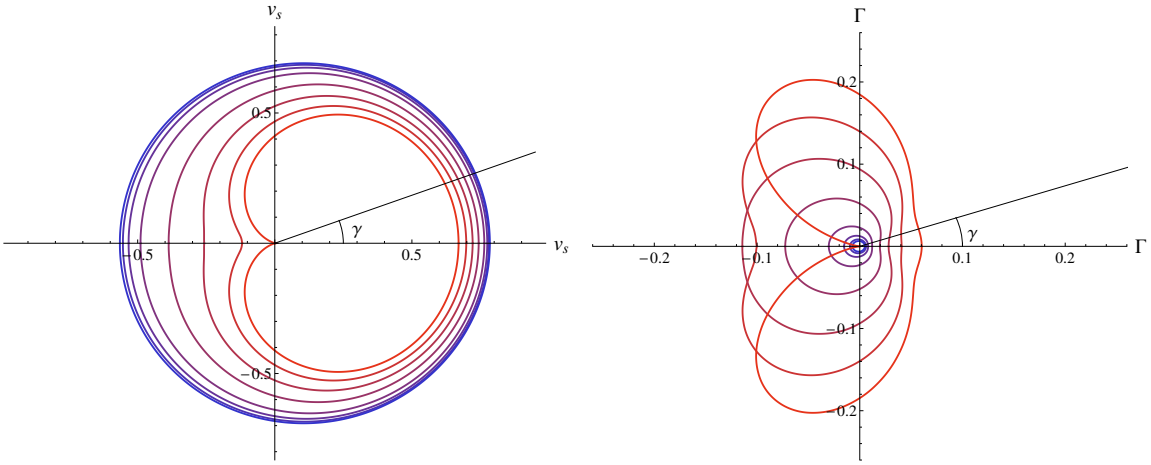

Figure 4. Sound velocity (left) and attenuation constant (right) for $S_x/\mu = 0.2$ as a function of the angle γ and for a range of temperatures from $T = 0.85T_c$ (red) to $T = 0.57T_c$ (blue).

used to obtain the hydrodynamic modes in coupled systems are well known. We will not elaborate on them here, referring the interested reader to [22] and [42].

In figures 3 and 4 we represent the velocity and the attenuation of the type I Goldstone mode. Its dispersion relation is given by (1.3) at low momentum, except now the speed of sound v_s and the attenuation constant Γ depend on the angle γ.[4] Figure 3 shows the angle dependent variation of the sound velocity and damping constant for a fixed temperature and varying values of the superfluid velocity. Figure 4 shows the same at fixed superfluid velocity but with varying temperature. As one would expect for small S_x/μ and low enough

[4]The small real constant b does not play a role here since for small enough momentum the linear part proportional to v_s dominates.

JHEP02(2014)063

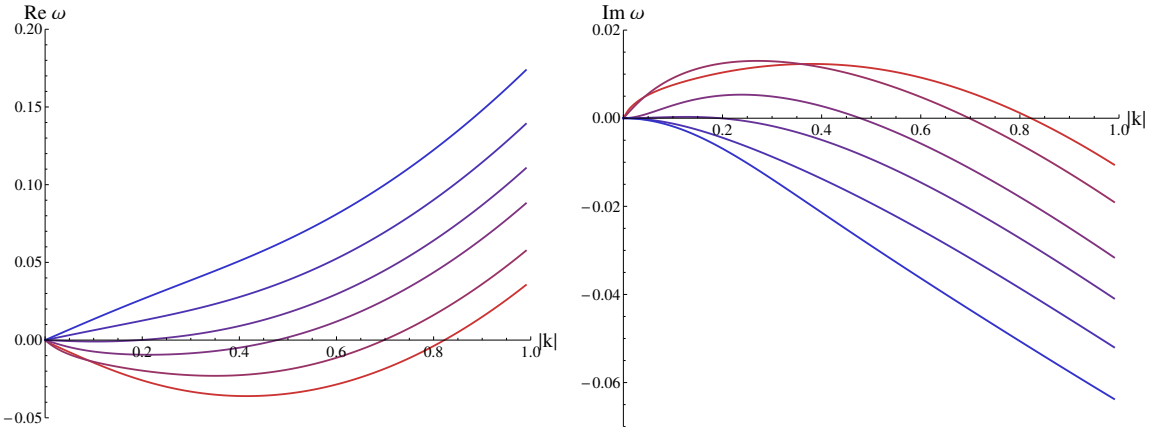

Figure 5. Real (left) and imaginary (right) parts of the frequency of the lowest hydrodynamic mode (type I Goldstone mode) versus momentum at $S_x/\mu = 0.1$ and $\gamma = \pi$ for different temperatures from $T = \tilde{T} = 0.970T_c$ (red) to $T = 0.905Tc$ (blue). The instability appears at $T^* = 0.935T_c$.

temperature the velocity and damping constant are almost isotropic. As the superfluid velocity is increased or the temperature is increased the plot becomes more and more asymmetric. The anisotropy of the system is such that we see an enhancement of the sound velocity and a reduction of the damping in the direction of the superflow.

The most interesting feature of the system is found however in the opposite direction to the superfluid velocity. As one can see in both plots, at $\gamma = \pi$ the reduction in the sound velocity is strongest and eventually both the attenuation constant and the sound velocity vanish simultaneously. It is important to stress that this happens below the temperature $\tilde{T}$. If one continues increasing the temperature (or equivalently increasing the superfluid velocity at fixed temperature) one finds that the real part of the frequency becomes negative and that its imaginary part crosses to the upper half plane, as depicted in figure 5. This signals the appearance of a tachyonic mode. T^* is the temperature where both the instability appears and the speed of sound becomes negative. This temperature actually signals the end of the superfluid phase according to the Landau criterion, and therefore we interpret it as the physical phase transition temperature.

In figure 6 (left) we present the phase diagram resulting from the QNM analysis. To illustrate the situation, on the right plot we show the behavior of the relevant QNM[5] at three different points of the phase diagram[6] (points labelled 1, 2, 3 on the left plot). At $\tilde{T} < T < T_c$ in the unbroken phase (line 3_N), the mode that was responsible for the transition to the homogeneous superfluid phase without superfluid velocity is shifted and becomes unstable at finite momentum. This behavior reflects the fact that the system is unstable for $T \leq T_c$, the mode being shifted in momentum due to the constant nonzero value of A_x. At $T = \tilde{T}$ (lines $2_{N,S}$) the lowest mode becomes unstable at $k = 0$. It is

[5]In the unbroken phase this is just the lowest scalar QNM, while in the broken phase it is the sound mode at fixed S_x/μ.

[6]An analogous discussion and phase space was found at weak coupling in [43] after the appearance of the first version of this paper.

JHEP02(2014)063

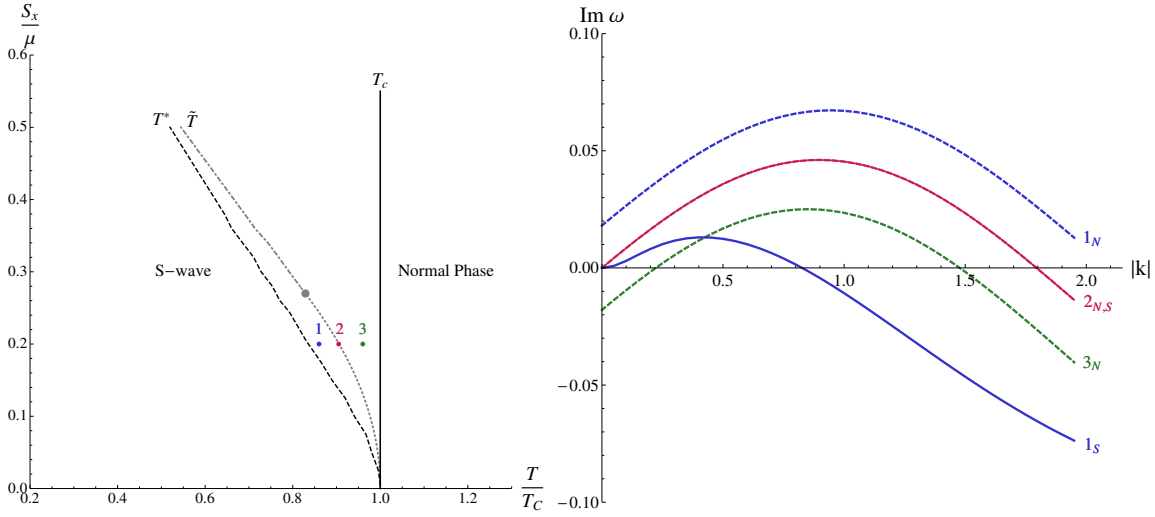

Figure 6. (Left) Phase diagram after the study of the QNMs. The grey dashed line corresponds to $\tilde{T}$, the apparent transition temperature found by direct analysis of the free energy. At a certain point (disk) the transition in free energy changes from 2nd order (dotted) to 1st order (dash-dotted). The black solid line corresponds to the critical temperature in absence of superfluid velocity. The black dashed line signals the physical phase transition at T^*, the temperature at which the local instability appears. Points 1, 2 and 3 indicate the values of temperature and velocity used in the plot on the right. (Right) Imaginary part of the lowest QNM for different temperatures at fixed $S_x/\mu = 0.2$ and $\gamma = \pi$. Dashed lines were obtained in the normal phase whereas solid lines were calculated in the superfluid phase.

at this point that the free energy of the homogeneous superfluid phase equals that of the normal phase. Hence, the free energy analysis, which only captures the $k = 0$ dynamics, predicts a phase transition at this temperature. For the particular superfluid velocity in the plot the phase transition is second order. Finally, the fate of the QNM for $T^* < T < \tilde{T}$ is shown in lines 1_N (for the normal phase) and 1_S (for the homogeneous superflow phase). One can see that the Goldstone mode in the superfluid phase is unstable for a finite range in momentum. Only at T^* this mode becomes stable again as shown in figure 5. It is at this temperature that the homogeneous superflow phase becomes stable according to the Landau criterion since the sound velocity becomes positive (moreover the imaginary part of the QNM dispersion relation lies entirely in the lower half plane).

Therefore the QNM results indicate that a phase transition occurs at a lower temperature $T^* < \tilde{T}$. Similarly, if we imagine the system at fixed temperature and start rising the superfluid velocity, both v_s and Γ will vanish at some value of S_x/μ, which we claim is indeed the critical velocity v_c of the superfluid, in the sense of the Landau criterion.

As a very interesting fact, notice that the imaginary part of the mode exhibiting the instability has a maximum at finite momentum as well. The fact that the instability appears at finite momentum suggests that there might exist a new (meta)stable intermediate phase above T^* with a spatially modulated condensate. Examples of such instabilities towards spatial modulation have been discussed before in [44–46].

JHEP02(2014)063

It is important to remark that, as shown in figure 6 (right), for temperatures $T^* < T < \tilde{T}$ the mode responsible for the transition to the (shifted) homogeneous stationary phase (line 1_N) and the new unstable mode (line 1_S) show maxima at different momenta. We take this as an indication for existence of a new metastable in-homogeneous phase. The wave number of the modulation in this phase should be determined by the maximum of the line 1_S.

Recall that the Landau criterion is formulated uniquely in terms of $\Re(\omega)$. At a given temperature the critical velocity corresponds to the superfluid velocity at which $v_s = 0$, or equivalently to the value of S_x/μ where $\Re(\omega)$ becomes negative (see figure 5). That the criterion is a statement about $\Re(\omega)$ reflects the fact that it holds also at zero temperature. At finite temperature the dispersion relation of the gapless mode gets itself altered due to both the superfluid velocity and the temperature [3, 39], implying that generically the critical value of S_x/μ at fixed temperature *does not* correspond to the velocity of sound at the same temperature and vanishing superfluid velocity.

An extra comment is in order here regarding the phase of the system for $T_c > T > \tilde{T}$. The fact that in the unbroken phase the lowest QNM is unstable in this regime (see line 3_N in figure 6) of course indicates that the normal phase is unstable. Let us comment on this. Since the condensate vanishes in the normal phase, there exists no physical notion of superfluid velocity in this phase; different choices of A_x are just different frame choices. In particular, a constant A_x simply acts as a shift in momentum in the unbroken phase, as can be seen from the fact that the maximum of the QNM is centered at a momentum equal to the value of the gauge field at the conformal boundary. Therefore the normal phase is unstable for any temperature lower than the critical temperature T_c towards the formation of a superfluid without superflow. On the other hand, we know that the homogeneous condensate solution with finite velocity does not exist in this region, and moreover it is unstable for $T > T^*$. We see two possibilities for the completion of the phase diagram in this region. First, the system could simply fall down to the true ground state, which is the condensate with no superflow. At finite S_x/μ this is still a solution which minimizes the energy albeit with a condensate that is not real anymore but rather has a space dependent phase such that $\vec{\nabla}\Phi = 0$. This is simply the gauge transformed homogeneous ground state without superflow. On the other hand, the fact that we found an instability at finite momentum in the temperature range $T^* < T < \tilde{T}$ could indicate that there is a spatially modulated (metastable) phase even in the range $T^* < T < T_c$, namely a striped superfluid. Due to the smooth appearance of the unstable mode we expect the transition at T^* to that phase to be 2nd order, although this should be studied in detail by constructing the correct inhomogeneous background. The explicit construction of this phase goes however substantially beyond the purpose of this paper and we leave this question open for further investigation.

3.1 Longitudinal conductivities in the U(1) sector

In this section we compute the conductivities in the $(0)-(3)$ sector in the presence of superfluid velocity. As far as we are aware, only the transverse conductivities have been computed so far (see for instance [16, 17]). In contrast, here we will focus on the longitudinal

JHEP02(2014)063

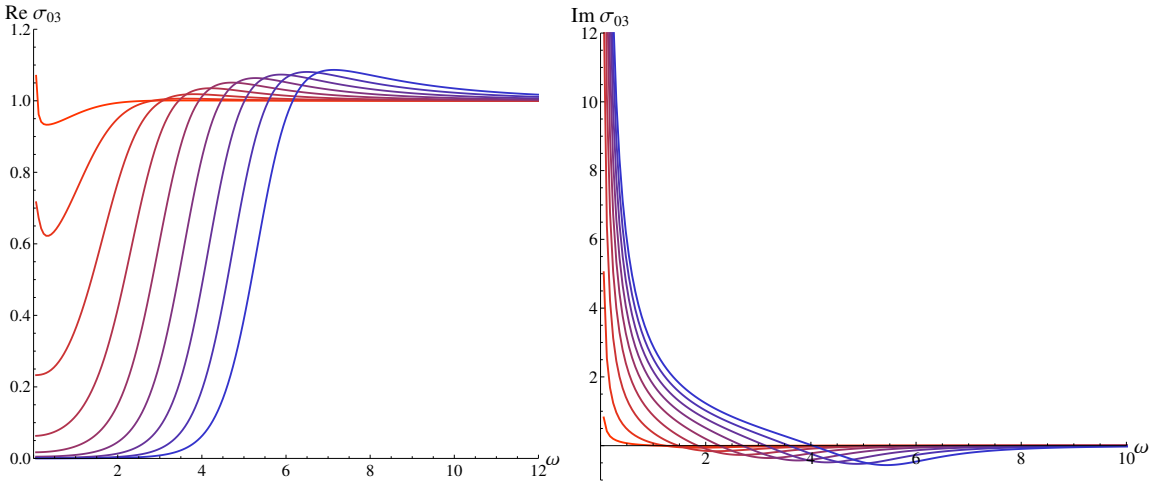

Figure 7. Plots of the Real (left) and Imaginary (right) parts of the conductivity for fixed $S_x/\mu = 0.05$. Different lines correspond to different temperatures from $T = 0.99T_c$(red) to $T = 0.38T_c$ (blue).

conductivities. These are calculated, via the Kubo formula

$$\sigma = \frac{i}{\omega}\langle J^x J^x \rangle \,, \tag{3.2}$$

from the two point function

$$\mathcal{G}_{IJ} = \lim_{\Lambda\to\infty} \left(\mathcal{A}_{IM}\mathcal{F}^M_{kJ}(\Lambda)'\right) , \tag{3.3}$$

where the matrix $\mathcal{A}$ can be read off from the on-shell action. $\mathcal{F}$ is the matrix valued bulk-to-boundary propagator normalized to the unit matrix at the boundary. Since we are only interested in the entry of the matrix corresponding to $\langle J^x J^x \rangle$ and the matrix $\mathcal{A}$ is diagonal, we just need one element, i.e. $\mathcal{A}_{xx} = -\frac{f(r)}{2}$. In order to construct the bulk-to-boundary propagator one needs a complete set of linearly independent solutions for the perturbations of the scalar and gauge fields. This implies solving the system of equations given in appendix A at zero momentum. The method follows closely the one detailed in [42]. Notice that there is a surviving coupling between the gauge fields and the scalar perturbations mediated by A_x. This makes the computation of the conductivities more involved than in the case without superflow.

Our results show little deviation from what was found at zero superflow. The most interesting new feature is a low frequency peak which appears due to the coupling between the gauge and the scalar sectors induced by the superfluid velocity. In figures 7 and 8 we present the results for different values of S_x/μ. As expected the behavior for small superfluid velocity far from the critical temperature is the same as the one obtained in [8]. Close to T^* a bump is generated in the real part of the conductivity at $\omega \approx 0$. This indicates the existence of a mode with very small imaginary gap. The mode responsible for this behavior is the pseudo-diffusive mode described in [22]. Due to the conserved U(1) symmetry of the unbroken phase, there exists a diffusive (gapless) mode in the QNM spectrum of the theory.

JHEP02(2014)063

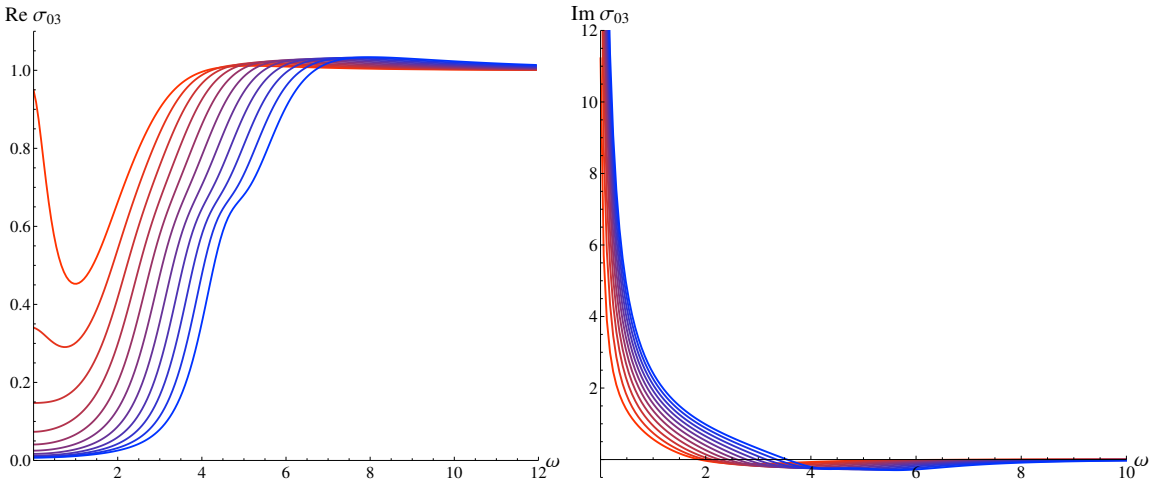

Figure 8. Real (left) and imaginary (right) parts of the conductivity for fixed $S_x/\mu = 0.4$. Different lines correspond to different temperatures in the range $T = 0.35T_c$ (blue)–$0.65T_c$ (red).

Once the symmetry is spontaneously broken, this mode develops a purely imaginary gap that increases as we lower the temperature. Therefore, for high enough temperatures below the phase transition, the gap of the pseudo-diffusive mode at $k = 0$ is very small and this implies the appearance of a peak at small frequencies in the conductivity as we can see in the figures. If we lower the temperature, the bump starts disappearing simply because the gap of the pseudo-diffusive mode becomes larger. Although this mode was already present in the analysis of the conductivities without superflow, it is only in our present case that it affects the conductivity, due to the coupling at zero momentum between the gauge and scalar sectors mediated by the field A_x. The size of the peak is proportional to the size of that coupling, i.e. it grows with S_x/μ.

4 Landau criterion for holographic Type II Goldstone bosons

In the previous section we studied the lowest lying QNM contained in the $(0)-(3)$ or U(1) sector of the theory for various values of the superfluid velocity and arbitrary angle between the momentum and the direction of the superflow. In this section we extend the analysis to the $(1)-(2)$ sector, which is particular of the U(2) model of [23] and contains a type II Goldstone boson in the spectrum, whose dispersion relation is given by (1.4) in the hydrodynamic limit.

The equations describing the system can be found in appendix B. In this case we choose the momentum to lie always in the direction opposite to the superflow, because as we will see this mode is always unstable. Along with the scalar perturbations described in (3.1) we have to consider the following gauge perturbations in the $(1)-(2)$ sector

$$\begin{aligned} A^{(1)} &= a_t^{(1)}(t,r,x)dt + a_x^{(1)}(t,r,x)dx\,, \\ A^{(2)} &= a_t^{(2)}(t,r,x)dt + a_x^{(2)}(t,r,x)dx\,. \end{aligned} \tag{4.1}$$

JHEP02(2014)063

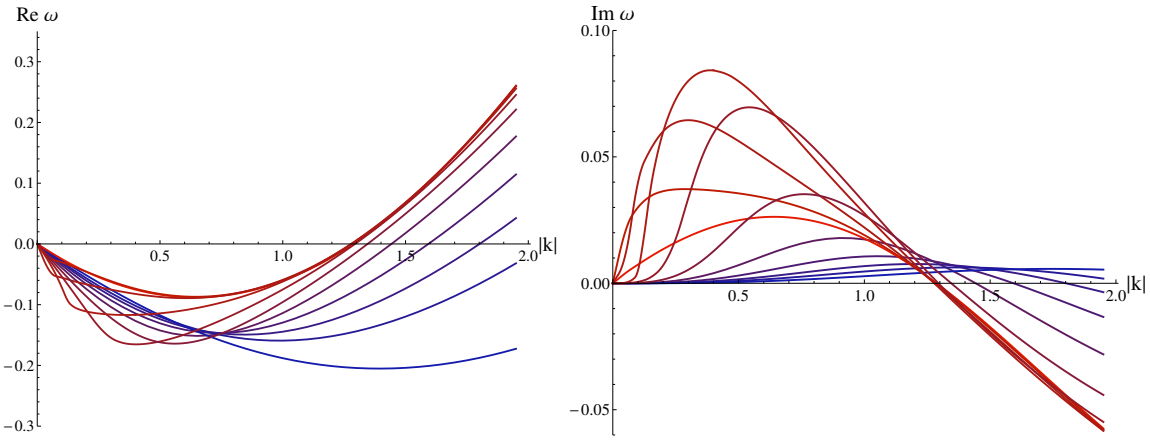

Figure 9. Real (left) and imaginary (right) parts of the dispersion relation of the lowest QNM of the $(1)-(2)$ sector in the gauged model for fixed $S_x/\mu = 0.15$ and a range of temperatures from $T = \tilde{T} = 0.95T_c$ (red) to $T = 0.45T_c$ (blue) and momentum anti-parallel to the superfluid velocity.

Again we use the determinant method of [42] to find the QNMs in this sector. Our results are summarized in figure 9, where the dispersion relation for the lowest QNM mode is shown at a particular superfluid velocity. We checked that the result is qualitatively the same for arbitrary S_x/μ.

The type II Goldstone mode becomes unstable for arbitrarily small superfluid velocities and temperatures below $\tilde{T}$. However, an important difference arises with respect to the U(1) sector. The tachyonic mode does not become stable at any temperature below $\tilde{T}$, contrary to the situation in the $(0)-(3)$ sector, there is no analogous of T^* in this sector. This behavior can be easily interpreted as a reflection of the Landau criterion of superfluidity in our holographic setup: according to (1.2), the critical velocity is zero in any system featuring type II Goldstone bosons, hence for any $T < \tilde{T}$ the superfluid phase is not stable at any finite superfluid velocity. In addition notice that the maximum in the imaginary part occurs at higher values of the momentum as we lower the temperature. In fact as we can see from the figure, lowering the temperature below $\tilde{T}$ the maximum in $\Im(\omega)$ first increases but then starts to decrease again as the temperature is lowered. At the same time it moves out to ever larger values of the momentum.

Note that plots analogous to figures 3 and 4 do not make any sense in the U(2) model, since the $(1)-(2)$ sector is unstable at any temperature we have been able to check.

4.1 Ungauged model

In [23] an ungauged model was defined in which there were no dynamical SU(2) gauge fields in the bulk. This model has a global SU(2) symmetry and a local U(1) symmetry. The dual field theory does therefore not possess the generators of the SU(2) symmetry in its operator spectrum. Nevertheless, as shown in [23] a somewhat unexpected type II Goldstone mode is present in the QNM spectrum of the model.

JHEP02(2014)063

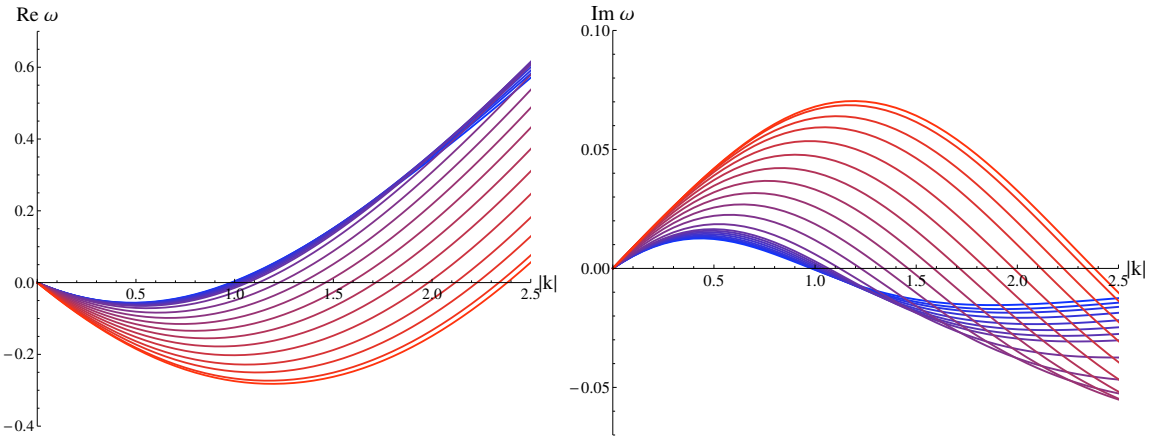

Figure 10. Real (left) and imaginary (right) parts of the dispersion relation of the lowest QNM in the (1)−(2) sector of the ungauged model for fixed $S_x/\mu = 0.25$ and a range of temperatures from $T = \tilde{T} = 0.853T_c$ (red) to $T = 0.306T_c$ (blue). Momentum is taken anti-parallel to the superfluid velocity.

The ungauged model is basically given by the same action (2.1) once we keep only the overall U(1) gauge field. Actually it corresponds to the simple U(1) model with two scalar fields with degenerate mass and therefore has an accidental SU(2) global symmetry.

The background solution is again that of the U(1) superfluid, hence the superflow solution can be accommodated also in the ungauged model. The difference is that the type II Goldstone mode appears now in the fluctuations of the upper component of the scalar field η, whose equation of motion reads

$$f\eta'' + \left(f' + \frac{2f}{r}\right)\eta' + \left(\frac{(\omega + A_0)^2}{f} - \frac{(k - A_x)^2}{r^2} - m^2\right)\eta = 0\,, \tag{4.2}$$

and is completely decoupled of all other field fluctuations. As noticed in [23] the change of the background due to the condensate is enough to trigger the appearance of the type II Goldstone.

It is remarkable that in the ungauged model the type II Goldstone mode is still unstable at any temperature below $\tilde{T}$ for any value of the superfluid velocity. Notice that not including conserved currents for the SU(2) symmetry, the model does not satisfy all theorems on existence of Goldstone bosons [23]. However, the Landau criterion of stability is still valid.

The ungauged model presents a qualitative difference with respect to the gauged model. The value of the momentum at the maximum now decreases as we lower the temperature. This is shown in figure 10, where the dispersion relation of the type II Goldstone at fixed superfluid velocity and for a long range of temperatures is plotted. For arbitrary values of the superfluid velocity we obtained analogous results.

JHEP02(2014)063

5 Conclusions

We have analyzed the holographic realization of the Landau criterion of superfluidity. The study was motivated by the appearance of type II Goldstone bosons in the model (2.1). The quadratic nature of the dispersion relation of the type II Goldstone mode should be responsible for driving the system out of the superfluid phase for arbitrarily small superfluid velocity.

Taking advantage of the fact that the usual U(1) holographic s-wave superconductor is contained in (2.1), we have revisited the Landau criterion for holographic type I Goldstone modes. When addressing the question of the stability of the condensate at finite superfluid velocity the analysis of the free energy does not give the correct answer. The QNM spectrum contains a tachyonic mode at finite momentum for temperatures $T^* < T < \tilde{T}$. As defined $\tilde{T}$ is the temperature at which free energies of the normal and condensate phase coincide. In contrast, T^* is the temperature where the tachyonic instability arises. Hence, the homogeneous superfluid is stable only for $T < T^*$, see figure 6. The results for the sound velocity as a function of the angle γ between the propagation direction and the superfluid velocity, depicted in figures 3 and 4, are perfectly consistent with this statement: at $T = T^*$ and $\gamma = \pi$ the velocity of sound vanishes. This condition can be seen to be equivalent to the Landau criterion and signals the existence of a critical velocity above which the superfluid is not stable anymore.

Since the maximum of the imaginary part of the unstable mode has non-vanishing wave number it is natural to suggest that there might be another, spatially modulated phase for $T > T^*$. The nature of this inhomogeneous phase is however unknown and we leave its explicit construction of even the question of its very existence for future research.

We have also computed the longitudinal conductivities for various superfluid velocities. As far as we know, they have not been computed before. We see a peak at $\omega = 0$, due to the coupling with the spatial component of the gauge field A_x. The peak decreases as we lower the temperature until it gets completely suppressed (figure 7). We believe that this enhancement of the DC conductivity is caused by the gap of the pseudo-diffusive mode [22, 23] which in the presence of superfluid velocity is formed due to the coupling between the gauge and scalar sectors that takes place even at $k = 0$.

Moving to the $(1) - (2)$ sector, we worked out the impact of the superflow on the type II Goldstone mode. We found that the Landau criterion is effective for arbitrarily small superfluid velocity as depicted in figure 9. The tachyon persists for the whole range of temperatures and (finite) superfluid velocities we have been able to analyze. Hence, we conclude that the critical superfluid velocity for this sector vanishes, in complete accordance with the Landau criterion applied to modes with dispersion relation $\omega \propto k^2$. An analogous result holds for the type II Goldstone mode in the ungauged model.

Acknowledgments

We have profited a lot from discussions with V. Giraldo and A. Schmitt. A.J. would like to thank Ioannis Papadimitriou for useful discussions. L.M. wants to thank the Imperial Col-

JHEP02(2014)063

lege London for their hospitality during his research visit, specially J.P. Gauntlett, C. Pantelidou and G. De Nadai Sowrey. This work has been supported by MEC and FEDER grant FPA2012-32828, Consolider Ingenio Programme CPAN (CSD2007-00042), Comunidad de Madrid HEP-HACOS S2009/ESP-1473 and MINECO Centro de excelencia Severo Ochoa Program under grant SEV-2012-0249. I.A. is supported by the Israel Science Foundation under grants no. 392/09 and 495/11. L.M. has been supported by FPI-fellowship BES-2010-041571. A.J. is supported by FPU fellowship AP2010-5686. D.A. thanks the FRont Of pro-Galician Scientists for unconditional support.

A Fluctuation equations in the $(0)-(3)$ sector

The fluctuations in the U(1) theory or the $(0)-(3)$ sector contain the zeroth and third color sectors of the gauge field and the lower component of the scalar field $\sigma = \rho + i\delta$. The equations of motion for an arbitrary direction of the momentum then read

$$0 = f\rho'' + \left(f' + \frac{2f}{r}\right)\rho' + \left(\frac{\omega^2}{f} + \frac{A_0^2}{f} - \frac{A_x^2}{r^2} - \frac{|k|^2}{r^2} - m^2\right)\rho + \frac{2i\omega A_0}{f}\delta + 2a_t^{(-)}\Psi\frac{A_0}{f} - 2\frac{a_x^{(-)}}{r^2}\Psi A_x + |k|\cos(\gamma)\frac{2i}{r^2}A_x\delta\,, \tag{A.1}$$

$$0 = f\delta'' + \left(f' + \frac{2f}{r}\right)\delta' + \left(\frac{\omega^2}{f} + \frac{A_0^2}{f} - \frac{A_x^2}{r^2} - \frac{|k|^2}{r^2} - m^2\right)\delta - \frac{2i\omega A_0}{f}\rho - i\Psi\omega\frac{a_t^{(-)}}{f} - |k|\cos(\gamma)\frac{2i}{r^2}A_x\rho - |k|\cos(\gamma)\frac{i}{r^2}\Psi a_x^{(-)} - |k|\sin(\gamma)\frac{i}{r^2}\Psi a_y^{(-)}, \tag{A.2}$$

$$0 = fa_t''^{(-)} + \frac{2f}{r}a_t'^{(-)} - \left(\frac{|k|^2}{r^2} + 2\Psi^2\right)a_t^{(-)} - \frac{\omega|k|}{r^2}\cos(\gamma)a_x^{(-)} - \frac{\omega|k|}{r^2}\sin(\gamma)a_y^{(-)} - 4\Psi A_0\rho - 2i\omega\Psi\delta\,, \tag{A.3}$$

$$0 = fa_x''^{(-)} + f'a_x'^{(-)} + \left(\frac{\omega^2}{f} - 2\Psi^2\right)a_x^{(-)} + \frac{\omega|k|}{f}\cos(\gamma)a_t^{(-)} + 2i|k|\cos(\gamma)\Psi\delta - 4\Psi\rho A_x - \frac{|k|^2\sin^2(\gamma)}{r^2}a_x^{(-)} + \frac{|k|^2\cos(\gamma)\sin(\gamma)}{r^2}a_y^{(-)}\,, \tag{A.4}$$

$$0 = fa_y''^{(-)} + f'a_y'^{(-)} + \left(\frac{\omega^2}{f} - 2\Psi^2\right)a_y^{(-)} + \frac{\omega|k|}{f}\sin(\gamma)a_t^{(-)} + 2i|k|\sin(\gamma)\Psi\delta - \frac{|k|^2\cos^2(\gamma)}{r^2}a_y^{(-)} + \frac{|k|^2\cos(\gamma)\sin(\gamma)}{r^2}a_x^{(-)}, \tag{A.5}$$

and the constraint

$$0 = \frac{i\omega}{f}a_t'^{(-)} + \frac{i|k|}{r^2}\cos(\gamma)a_x'^{(-)} + \frac{i|k|}{r^2}\sin(\gamma)a_y'^{(-)} + 2\Psi'\delta - 2\Psi\delta', \tag{A.6}$$

where we have used $k_x = |k|\cos(\gamma)$, $k_y = |k|\sin(\gamma)$. The general pure gauge solution in this sector is

$$\delta = i\lambda\Psi\,; \qquad \rho = 0\,; \qquad a_t^{(-)} = \lambda\omega\,; \qquad a_x^{(-)} = -\lambda|k|\cos(\gamma)\,; \qquad a_y^{(-)} = -\lambda|k|\sin(\gamma)\,, \tag{A.7}$$

where λ is an arbitrary constant.

B Fluctuation equations in the (1)−(2) sector

The perturbations in the (1)−(2) sector of the U(2) theory include the fluctuations of the upper component of the scalar field, $\eta = \alpha + i\beta$, along with that sector of the gauge field. For momentum in the opposite direction of the superflow, the equations of motion read

$$0 = f a_x^{\prime\prime(1)} + f' a_x^{\prime(1)} + \left(\frac{\omega^2}{f} - \Psi^2 + \frac{(A_t^{(3)})^2}{f}\right) a_x^{(1)} - 2i\frac{A_t^{(3)}\omega}{f} a_x^{(2)} + i\omega\frac{A_x^{(3)}}{f} a_t^{(2)} - \frac{A_t^{(3)} A_x^{(3)}}{f} a_t^{(1)} - 2A_x^{(0)}\Psi\alpha + 2ik\Psi\beta - \frac{ikA_t^{(3)}}{f} a_t^{(2)} + \frac{\omega k}{f} a_t^{(1)}, \tag{B.1}$$

$$0 = f a_x^{\prime\prime(2)} + f' a_x^{\prime(2)} + \left(\frac{\omega^2}{f} - \Psi^2 + \frac{(A_t^{(3)})^2}{f}\right) a_x^{(2)} + 2i\frac{A_t^{(3)}\omega}{f} a_x^{(1)} - i\omega\frac{A_x^{(3)}}{f} a_t^{(1)} - \frac{A_t^{(3)} A_x^{(3)}}{f} a_t^{(2)} + 2\Psi A_x^{(0)}\beta + 2ik\Psi\alpha + \frac{ikA_t^{(3)}}{f} a_t^{(1)} + \frac{\omega k}{f} a_t^{(2)}, \tag{B.2}$$

$$0 = f a_t^{\prime\prime(1)} + \frac{2f}{r} a_t^{\prime(1)} - \left(\frac{(A_x^{(3)})^2}{r^2} + \Psi^2 + \frac{k^2}{r^2}\right) a_t^{(1)} + \frac{A_t^{(3)} A_x^{(3)}}{r^2} a_x^{(1)} - i\omega\frac{A_x^{(3)}}{r^2} a_x^{(2)} - 2i\omega\beta\Psi - 2\phi\Psi\alpha + \frac{ikA_t^{(3)}}{r^2} a_x^{(2)} - \frac{2ikA_x^{(3)}}{r^2} a_t^{(2)} - \frac{\omega k}{r^2} a_x^{(1)}, \tag{B.3}$$

$$0 = f a_t^{\prime\prime(2)} + \frac{2f}{r} a_t^{\prime(2)} - \left(\frac{(A_x^{(3)})^2}{r^2} + \Psi^2 + \frac{k^2}{r^2}\right) a_t^{(2)} + \frac{A_t^{(3)} A_x^{(3)}}{r^2} a_x^{(2)} + i\omega\frac{A_x^{(3)}}{r^2} a_x^{(1)} - \frac{ikA_t^{(3)}}{r^2} a_x^{(1)} + \frac{2ikA_x^{(3)}}{r^2} a_t^{(1)} - \frac{\omega k}{r^2} a_x^{(2)} - 2i\omega\alpha\Psi + 2A_t^{(0)}\Psi\beta\,, \tag{B.4}$$

$$0 = f\alpha'' + \left(f' + \frac{2f}{r}\right)\alpha' + \left(\frac{\omega^2}{f} + \frac{(A_t^{(0)} + A_t^{(3)})^2}{4f} - \frac{(A_x^{(0)} + A_x^{(3)})^2}{4r^2} - \frac{k^2}{r^2} - m^2\right)\alpha + \left(i\omega\left(\frac{A_t^{(0)} + A_t^{(3)}}{f}\right) + \frac{ik}{r^2}(A_x^{(0)} + A_x^{(3)})\right)\beta + \frac{A_t^{(0)}\Psi}{2f} a_t^{(1)} - i\omega\frac{\Psi}{2f} a_t^{(2)} - \frac{A_x^{(0)}\Psi}{2r^2} a_x^{(1)} - \frac{ik\Psi}{2r^2} a_x^{(2)}, \tag{B.5}$$

$$0 = f\beta'' + \left(f' + \frac{2f}{r}\right)\beta' + \left(\frac{\omega^2}{f} + \frac{(A_t^{(0)} + A_t^{(3)})^2}{4f} - \frac{(A_x^{(0)} + A_x^{(3)})^2}{4r^2} - \frac{k^2}{r^2} - m^2\right)\beta - \left(i\omega\left(\frac{A_t^{(0)} + A_t^{(3)}}{f}\right) + \frac{ik}{r^2}(A_x^{(0)} + A_x^{(3)})\right)\alpha - \frac{A_t^{(0)}\Psi}{2f} a_t^{(2)} - i\omega\frac{\Psi}{2f} a_t^{(1)} + \frac{A_x^{(0)}\Psi}{2r^2} a_x^{(2)} - \frac{ik\Psi}{2r^2} a_x^{(1)}, \tag{B.6}$$

subject to the constraints

$$0 = 2f(\Psi\beta' - \Psi'\beta) + a_t^{(2)} A_t^{\prime(3)} - a_t^{\prime(2)} A_t^{(3)} + \frac{f}{r^2}(A_x^{(3)} a_x^{\prime(2)} - a_x^{(2)} A_x^{\prime(3)}) - i\omega a_t^{\prime(1)} - \frac{ikf}{r^2} a_x^{\prime(1)}, \tag{B.7}$$

$$0 = 2f(\Psi\alpha' - \Psi'\alpha) + a_t^{\prime(1)} A_t^{(3)} - a_t^{(1)} A_t^{\prime(3)} + \frac{f}{r^2}(a_x^{(1)} A_x^{\prime(3)} - A_x^{(3)} a_x^{\prime(1)}) - i\omega a_t^{\prime(2)} - \frac{ikf}{r^2} a_x^{\prime(2)}, \tag{B.8}$$

There are two pure gauge solutions in this sector,

$$\alpha = 0\,, \qquad \beta = i\lambda_1\Psi/2\,, \quad a_t^{(1)} = \lambda_1\omega\,, \qquad a_t^{(2)} = i\lambda_1 A_t^{(3)}, \quad a_x^{(1)} = -\lambda_1 k\,, \qquad a_x^{(2)} = i\lambda_1 A_x^{(3)}, \tag{B.9}$$

$$\alpha = i\lambda_2\Psi/2\,, \quad \beta = 0\,, \qquad a_t^{(1)} = -i\lambda_2 A_t^{(3)}, \quad a_t^{(2)} = \lambda_2\omega\,, \qquad a_x^{(1)} = -i\lambda_2 A_x^{(3)}, \quad a_x^{(2)} = -\lambda_2 k\,, \tag{B.10}$$

where λ_1 and λ_2 are arbitrary constants.

References

[1] L. Landau and E.M. Lifshitz, *Course of theoretical physics, volume 5*, Elsevier (2008).

[2] I. Khalatnikov, *An introduction to the theory of superfluidity*, Advanced Book Classics, Perseus Books (2000).

[3] D. Pines and P. Nozières, *The theory of quantum liquids*, Advanced Book Classics, Perseus Books (1999).

[4] S.A. Hartnoll, *Lectures on holographic methods for condensed matter physics*, *Class. Quant. Grav.* **26** (2009) 224002 [arXiv:0903.3246] [INSPIRE].

[5] C.P. Herzog, *Lectures on holographic superfluidity and superconductivity*, *J. Phys.* **A 42** (2009) 343001 [arXiv:0904.1975] [INSPIRE].

[6] J. McGreevy, *Holographic duality with a view toward many-body physics*, *Adv. High Energy Phys.* **2010** (2010) 723105 [arXiv:0909.0518] [INSPIRE].

[7] S.S. Gubser, *Breaking an Abelian gauge symmetry near a black hole horizon*, *Phys. Rev.* **D 78** (2008) 065034 [arXiv:0801.2977] [INSPIRE].

[8] S.A. Hartnoll, C.P. Herzog and G.T. Horowitz, *Building a holographic superconductor*, *Phys. Rev. Lett.* **101** (2008) 031601 [arXiv:0803.3295] [INSPIRE].

[9] S.A. Hartnoll, C.P. Herzog and G.T. Horowitz, *Holographic superconductors*, *JHEP* **12** (2008) 015 [arXiv:0810.1563] [INSPIRE].

[10] S.S. Gubser and S.S. Pufu, *The gravity dual of a p-wave superconductor*, *JHEP* **11** (2008) 033 [arXiv:0805.2960] [INSPIRE].

[11] M. Ammon, J. Erdmenger, M. Kaminski and P. Kerner, *Superconductivity from gauge/gravity duality with flavor*, *Phys. Lett.* **B 680** (2009) 516 [arXiv:0810.2316] [INSPIRE].

[12] F. Benini, C.P. Herzog, R. Rahman and A. Yarom, *Gauge gravity duality for d-wave superconductors: prospects and challenges*, *JHEP* **11** (2010) 137 [arXiv:1007.1981] [INSPIRE].

[13] J.-W. Chen, Y.-J. Kao, D. Maity, W.-Y. Wen and C.-P. Yeh, *Towards a holographic model of D-wave superconductors*, *Phys. Rev.* **D 81** (2010) 106008 [arXiv:1003.2991] [INSPIRE].

[14] C.P. Herzog, P. Kovtun and D. Son, *Holographic model of superfluidity*, *Phys. Rev.* **D 79** (2009) 066002 [arXiv:0809.4870] [INSPIRE].

JHEP02(2014)063

[15] P. Basu, A. Mukherjee and H.-H. Shieh, *Supercurrent: vector hair for an AdS black hole*, *Phys. Rev.* **D 79** (2009) 045010 [arXiv:0809.4494] [INSPIRE].

[16] D. Arean, P. Basu and C. Krishnan, *The many phases of holographic superfluids*, *JHEP* **10** (2010) 006 [arXiv:1006.5165] [INSPIRE].

[17] D. Arean, M. Bertolini, J. Evslin and T. Prochazka, *On holographic superconductors with DC current*, *JHEP* **07** (2010) 060 [arXiv:1003.5661] [INSPIRE].

[18] G.T. Horowitz and V.E. Hubeny, *Quasinormal modes of AdS black holes and the approach to thermal equilibrium*, *Phys. Rev.* **D 62** (2000) 024027 [hep-th/9909056] [INSPIRE].

[19] D. Birmingham, I. Sachs and S.N. Solodukhin, *Conformal field theory interpretation of black hole quasinormal modes*, *Phys. Rev. Lett.* **88** (2002) 151301 [hep-th/0112055] [INSPIRE].

[20] E. Berti, V. Cardoso and A.O. Starinets, *Quasinormal modes of black holes and black branes*, *Class. Quant. Grav.* **26** (2009) 163001 [arXiv:0905.2975] [INSPIRE].

[21] K. Landsteiner, *The sound of strongly coupled field theories: quasinormal modes in AdS*, *AIP Conf. Proc.* **1458** (2011) 174 [arXiv:1202.3550] [INSPIRE].

[22] I. Amado, M. Kaminski and K. Landsteiner, *Hydrodynamics of holographic superconductors*, *JHEP* **05** (2009) 021 [arXiv:0903.2209] [INSPIRE].

[23] I. Amado et al., *Holographic type II Goldstone bosons*, *JHEP* **07** (2013) 108 [arXiv:1302.5641] [INSPIRE].

[24] A. Krikun, V. Kirilin and A. Sadofyev, *Holographic model of the $S^{\pm}$ multiband superconductor*, *JHEP* **07** (2013) 136 [arXiv:1210.6074] [INSPIRE].

[25] B.I. Halperin, *Dynamic properties of the multicomponent Bose fluid*, *Phys. Rev.* **B 11** (1975) 178.

[26] T. Brauner, *Spontaneous symmetry breaking and Nambu-Goldstone bosons in quantum many-body systems*, *Symmetry* **2** (2010) 609 [arXiv:1001.5212] [INSPIRE].

[27] V. Miransky and I. Shovkovy, *Spontaneous symmetry breaking with abnormal number of Nambu-Goldstone bosons and kaon condensate*, *Phys. Rev. Lett.* **88** (2002) 111601 [hep-ph/0108178] [INSPIRE].

[28] T. Schäfer, D. Son, M.A. Stephanov, D. Toublan and J. Verbaarschot, *Kaon condensation and Goldstone's theorem*, *Phys. Lett.* **B 522** (2001) 67 [hep-ph/0108210] [INSPIRE].

[29] H. Watanabe and H. Murayama, *Redundancies in Nambu-Goldstone bosons*, *Phys. Rev. Lett.* **110** (2013) 181601 [arXiv:1302.4800] [INSPIRE].

[30] A. Kapustin, *Remarks on nonrelativistic Goldstone bosons*, arXiv:1207.0457 [INSPIRE].

[31] H. Watanabe, T. Brauner and H. Murayama, *Massive Nambu-Goldstone bosons*, *Phys. Rev. Lett.* **111** (2013) 021601 [arXiv:1303.1527] [INSPIRE].

[32] A. Nicolis and F. Piazza, *A relativistic non-relativistic Goldstone theorem: gapped Goldstones at finite charge density*, *Phys. Rev. Lett.* **110** (2013) 011602 [arXiv:1204.1570] [INSPIRE].

[33] A. Nicolis, R. Penco, F. Piazza and R.A. Rosen, *More on gapped Goldstones at finite density: more gapped Goldstones*, *JHEP* **11** (2013) 055 [arXiv:1306.1240] [INSPIRE].

[34] V.G. Filev, C.V. Johnson and J.P. Shock, *Universal holographic chiral dynamics in an external magnetic field*, *JHEP* **08** (2009) 013 [arXiv:0903.5345] [INSPIRE].

JHEP02(2014)063

[35] P. Basu, J. He, A. Mukherjee, M. Rozali and H.-H. Shieh, *Competing holographic orders*, *JHEP* **10** (2010) 092 [arXiv:1007.3480] [INSPIRE].

[36] R.-G. Cai, L. Li, L.-F. Li and Y.-Q. Wang, *Competition and coexistence of order parameters in holographic multi-band superconductors*, *JHEP* **09** (2013) 074 [arXiv:1307.2768] [INSPIRE].

[37] D. Musso, *Competition/enhancement of two probe order parameters in the unbalanced holographic superconductor*, *JHEP* **06** (2013) 083 [arXiv:1302.7205] [INSPIRE].

[38] V. Keranen, E. Keski-Vakkuri, S. Nowling and K. Yogendran, *Solitons as probes of the structure of holographic superfluids*, *New J. Phys.* **13** (2011) 065003 [arXiv:1012.0190] [INSPIRE].

[39] M.G. Alford, S.K. Mallavarapu, A. Schmitt and S. Stetina, *From a complex scalar field to the two-fluid picture of superfluidity*, *Phys. Rev.* **D 87** (2013) 065001 [arXiv:1212.0670] [INSPIRE].

[40] H. Watanabe and T. Brauner, *On the number of Nambu-Goldstone bosons and its relation to charge densities*, *Phys. Rev.* **D 84** (2011) 125013 [arXiv:1109.6327] [INSPIRE].

[41] I.R. Klebanov and E. Witten, *AdS/CFT correspondence and symmetry breaking*, *Nucl. Phys.* **B 556** (1999) 89 [hep-th/9905104] [INSPIRE].

[42] M. Kaminski, K. Landsteiner, J. Mas, J.P. Shock and J. Tarrio, *Holographic operator mixing and quasinormal modes on the brane*, *JHEP* **02** (2010) 021 [arXiv:0911.3610] [INSPIRE].

[43] M.G. Alford, S.K. Mallavarapu, A. Schmitt and S. Stetina, *Role reversal in first and second sound in a relativistic superfluid*, arXiv:1310.5953 [INSPIRE].

[44] S. Nakamura, H. Ooguri and C.-S. Park, *Gravity dual of spatially modulated phase*, *Phys. Rev.* **D 81** (2010) 044018 [arXiv:0911.0679] [INSPIRE].

[45] A. Donos and J.P. Gauntlett, *Holographic striped phases*, *JHEP* **08** (2011) 140 [arXiv:1106.2004] [INSPIRE].

[46] C.B. Bayona, K. Peeters and M. Zamaklar, *A non-homogeneous ground state of the low-temperature Sakai-Sugimoto model*, *JHEP* **06** (2011) 092 [arXiv:1104.2291] [INSPIRE].

JHEP02(2014)063